A Decentralized Guaranteed Collision Avoidance Control Framework for Multi-Vehicle Systems in Highly Constrained Spaces

Erick J. Rodríguez-Seda[a]

Department of Weapons, Robotics, and Control Engineering,
United States Naval Academy, Annapolis, MD, U.S.A.

Abstract: Collision avoidance methods based on artificial potential field functions generally assume vehicles and obstacles to have circular or elliptical shapes, which hinders mobility through narrow and cluttered spaces. To counteract this problem, this paper presents a decentralized, cooperative control framework for vehicles of unicycle type that considers the non-circular shape and relative orientation of vehicles and obstacles, increasing their maneuverability through tight spaces. The control framework proposes the use of a continuously differentiable time-varying minimum safe distance that agents need to enforce based on their shape and relative orientation and modulates the avoidance maneuvers and reaction forces based on the collision threat, increasing the reaction forces when the vehicles are fast approaching and relaxing the forces when they are moving away. The resulting closed-form control inputs are continuously smooth and bounded and are rigorously proven to guarantee collision avoidance at all times.

1 INTRODUCTION

Nowadays, unmanned vehicles operate in complex and dynamic environments such as disaster relief zones, border control, and warehouses, to name a few. Oftentimes, they need to navigate through highly constrained zones while sharing the space with other vehicles and obstacles. The latter tends to compromise mobility in lieu of safety (Xiao et al., 2021). Therefore, it is mission-critical to design control algorithms that allow these vehicles to have higher mobility and performance while maintaining safety.

1.1 Related Work

Collision avoidance control algorithms for unmanned vehicles have been studied for decades (Hoy et al., 2014; Raibail et al., 2022). They typically lie in one of two categories: motion planning and reactive control. Motion planning methods can lead to optimal trajectories, but their implementation is mostly centralized, demanding information from all other agents, or requires an accurate model of the environment (Hoy et al., 2014). Real-time reactive collision avoidance methods, on the other hand, can be decentralized and respond to unexpected obstacles, making these strategies more suitable for unknown and dynamic spaces.

A popular branch among real-time reactive control methods is the use of artificial potential field (APF) functions (Khatib, 1986). APF-based methods allow one to build provably safe collision avoidance control laws that can not only guarantee safety but can be implemented in a decentralized way and for an arbitrarily large number of vehicles (Stipanović et al., 2007). Recent examples of decentralized methods for multi-vehicle systems include (Du et al., 2019; Melchiorre et al., 2022; Gao et al., 2024). Yet, most APF-based approaches rely on the conservative assumption that agents, that is, vehicles and obstacles, are of circular or elliptical shape, or a collection of them (Stipanović et al., 2007; Braquet and Bakolas, 2022). This worst-case scenario assumption simplifies the analysis at the expense of making the agents occupy a larger space. For instance, consider the two vehicles of rectangular shape in Figure 1. The circular body assumption will require both vehicles to keep a distance from each other equal to or larger than the summation of their circumradii, $r_{ij}^{max} = h_i + h_j$, regardless of their relative orientation. Instead, one could take their shape and orientation into consideration and reduce the distance, r_{ij}, that agents need to keep from each other, as shown in Figure 1. A recent APF-based approach that takes into consideration their orientation and shape is presented in (Rodríguez-Seda, 2024b).

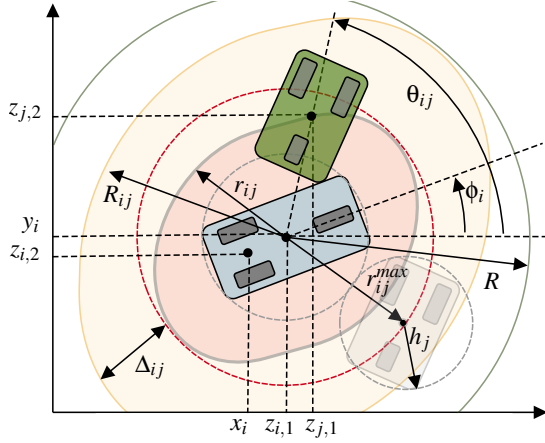[a] https://orcid.org/0000-0003-1108-4329

Figure 1: Minimum safe distance. Traditional approaches assume vehicles to have circular shapes and enforce a constant minimum distance equal to or greater than the sum of their circumradii $r_{ij}^{max} = h_i + h_j$.

Another common drawback of most APF-based methods is the equal treatment of obstacles that are moving away and those approaching. This is due to the sole reliance on relative position among agents while ignoring the direction of motion or velocity. Recent research efforts that integrate relative velocity information into the APF formulation include (Zhang et al., 2020; Ginesi et al., 2021). These approaches, however, require the obstacle's velocity, which might not be available or difficult to estimate. As an alternative, the work in (Rodríguez-Seda and Stipanović, 2020; Rodríguez-Seda, 2024a) proposes an APF-based framework that only uses the vehicle's velocity information and not the obstacle's, relaxing the APF force if the vehicle is moving away from the obstacle and increasing it if the vehicle is moving closer to it.

1.2 Contributions

This paper builds on (Rodríguez-Seda and Stipanović, 2020) and (Rodríguez-Seda, 2024b) to propose a decentralized, cooperative APF-based control law for nonholonomic vehicles of unicycle type that guarantees collision avoidance at all times while increasing maneuverability through dynamic and highly cluttered spaces. The proposed control law takes into consideration the shape and relative orientation of vehicles and obstacles to yield non-circular, tighter avoidance zones. In contrast to other collision avoidance methods for non-circular obstacles (Zimmermann et al., 2022), the proposed framework yields closed-form controllers that generate smooth and continuous forces and torques. Furthermore, the vehicle's avoidance response is modulated based on the collision threat: it increases or decreases the repul-

sive force and activation distance if the vehicle is approaching the obstacle or moving away. To demonstrate the performance of the control framework, a simulation example is presented and compared with the use of constant avoidance and reaction zones.

2 PROBLEM

2.1 Multi-Vehicle System Dynamics

Consider a group of N nonholonomic vehicles of unicycle type with dynamic equations governed by

$$\dot{x}_i(t) = v_i(t)\cos\phi_i(t), \qquad m_i\dot{v}_i(t) = f_i(t)$$
$$\dot{y}_i(t) = v_i(t)\sin\phi_i(t), \qquad J_i\dot{\omega}_i(t) = \tau_i(t) \qquad (1)$$
$$\dot{\phi}_i(t) = \omega_i(t),$$

where $x_i(t)$ and $y_i(t)$ are the position coordinates, $\phi_i(t)$ is the orientation, $v_i(t)$ and $\omega_i(t)$ are the linear and angular velocities, m_i is the mass, J_i is the inertia, and $f_i(t)$ and $\tau_i(t)$ are the control force and torque inputs for the ith robot (see Figure 1). The control objective is to design[1] f_i and τ_i such that the ith vehicle follows a desired path while avoiding collisions with other vehicles and obstacles. Unfortunately, it is well known that the position and orientation of (1) cannot be simultaneously stabilized at a desired value using a continuous static state feedback control law (Brockett, 1983). Therefore, this paper proposes the use of input-output feedback linearization, where the control task shifts to regulating the position of a *reference point* in front of (x_i, y_i) given by

$$z_{i,1} = x_i + L_i\cos\phi_i, \qquad z_{i,2} = y_i + L_i\sin\phi_i \quad (2)$$

where $L_i > 0$ is a constant parameter and $\mathbf{z}_i = [z_{i,1}, z_{i,2}]^T$ are the Cartesian coordinates of the reference point. Now, differentiating twice equation (2) and applying the following control force and torque

$$
\begin{bmatrix} f_i \\ \tau_i \end{bmatrix} =
\begin{bmatrix}
\dfrac{\cos\phi_i}{m_i} & \dfrac{\sin\phi_i}{m_i} \\
\dfrac{-\sin\phi_i}{J_iL_i} & \dfrac{\cos\phi_i}{J_iL_i}
\end{bmatrix}
$$
$$
\times
\begin{bmatrix}
u_{i,1} + v_i\omega_i\sin\phi_i + L_i\omega_i^2\cos\phi_i \\
u_{i,2} - v_i\omega_i\cos\phi_i + L_i\omega_i^2\sin\phi_i
\end{bmatrix} \quad (3)
$$

one can show that (1) reduces to

$$\ddot{\mathbf{z}}_i = \mathbf{u}_i \qquad (4a)$$

$$\dot{\phi}_i = L_i^{-1} \begin{bmatrix} -\sin\phi_i L_i & \cos\phi_i L_i \end{bmatrix} \dot{\mathbf{z}}_i \qquad (4b)$$

where $\mathbf{u}_i = [u_{i,1}, u_{i,2}]^T$ is the new control input for the linearized system. While the internal dynamics (4b)

---

[1]In what follows, the time argument of signals will be omitted unless it is deemed necessary.

can only be shown to be Lagrange stable (Rodríguez-Seda et al., 2014), the linear dynamics of the reference point (4a) are controllable. That is, for a any desired position $\mathbf{z}_i^d \in \mathbb{R}^2$, one can design a state feedback control law $\mathbf{u}_i$ such that $\mathbf{z}_i \to \mathbf{z}_i^d$ as $t \to \infty$.

2.2 Problem Formulation

The main control objective is to design a decentralized cooperative control framework that guarantees the safe navigation of multiple vehicles through highly constrained spaces. To this end, consider the interaction of a pair of agents ith and jth, as illustrated in Figure 1. Note that the *minimum safe distance* (or envelope) between the agents, denoted as r_{ij}, is not only a function of their shapes and dimensions but also of their relative position and orientations

$$r_{ij} := r_{ij}(\mathbf{z}_i - \mathbf{z}_j, \phi_i, \phi_j) = r_{ji}(\mathbf{z}_j - \mathbf{z}_i, \phi_j, \phi_i). \quad (5)$$

That is, r_{ij} depends on how the jth agent or obstacle is positioned with respect to the ith vehicle. One then says that a collision takes place if $\|\mathbf{z}_i - \mathbf{z}_j\| \le r_{ij}$ for some time t. In what follows, it is assumed that one can find an envelop function r_{ij} that is continuously differentiable with bounded derivative. Finally, it is assumed that the vehicles can detect, either via communication or onboard sensors, the relative position and orientation of other agents within a bounded *detection radius* $R > \sup_{i,j \ne i}\{r_{ij}\} = r_{ij}^{max}$.

Having defined the minimum safe distance and the detection radius, one can formulate the control objective as follows. Design a control strategy $\mathbf{u}_i$ such that $\mathbf{z}_i \to \mathbf{z}_i^d$ as $t \to \infty$ and $\|\mathbf{z}_i - \mathbf{z}_j\| > r_{ij}\ \forall\ i, j \ne i, t \ge 0$, where $\mathbf{z}_i^d$ is the desired final position.

3 CONTROL FRAMEWORK

3.1 Collision Avoidance Control

To achieve the control objective, this paper proposes the use of the following control law

$$\mathbf{u}_i = K_p(\mathbf{z}_i^d - \mathbf{z}_i) - K_v \dot{\mathbf{z}}_i + \mathbf{u}_i^a \quad (6)$$

where K_v and K_p are positive constants and $\mathbf{u}_i^a$ is the collision avoidance control input given by

$$\mathbf{u}_i^a = -\sum_{j \in N_i}\left(\frac{\partial V_{ij}^T}{\partial \mathbf{z}_i} + \frac{\partial V_{ij}^0}{\partial r_{ij}}\frac{\partial r_{ij}}{\partial \mathbf{z}_i}^T + \frac{1}{L_i}\frac{\partial V_{ij}^0}{\partial r_{ij}}\frac{\partial r_{ij}}{\partial \phi_i}\begin{bmatrix} -\sin\phi_i \\ \cos\phi_i \end{bmatrix}\right) \quad (7)$$

The group $N_i = \{j \in \{1, \cdots, N\}/i, \|\mathbf{z}_i - \mathbf{z}_j\| \le R\}$ is the set of neighbors of the ith agent and V_{ij} and V_{ij}^0 are avoidance functions (Stipanović et al., 2007) given by

$$V_{ij} := V_{ij}(\mathbf{z}_i, \mathbf{z}_j, r_{ij}, R_{ij}) = \left(\min\left\{0, \frac{\|\mathbf{z}_i - \mathbf{z}_j\|^2 - R_{ij}^2}{\|\mathbf{z}_i - \mathbf{z}_j\|^2 - r_{ij}^2}\right\}\right)^2$$

$$V_{ij}^0 := V_{ij}(\mathbf{z}_i, \mathbf{z}_j, r_{ij}, R_{ij}^0). \quad (8)$$

The *reaction radius* R_{ij} represents the distance at which the ith vehicle starts avoiding the jth agent. Ideally, this radius should be larger if the ith vehicle is approaching the jth agent at a large speed and smaller if it is moving away. Therefore, similar to (Rodríguez-Seda and Stipanović, 2020), this paper proposes the use of

$$R_{ij} := R_{ij}(\lambda_{ij}) = r_{ij} + \Delta_{ij}(\lambda_{ij}) \quad (9a)$$

$$\Delta_{ij} := \Delta_{ij}(\lambda_{ij}) = \bar{\Delta}\left(\frac{1}{2} + \frac{\tan^{-1}(\alpha\lambda_{ij} + \sigma)}{\pi}\right) \quad (9b)$$

where Δ_{ij} denotes the *reaction gap distance* (i.e., the distance at which the ith vehicle starts reacting to obstacles), $0 < \bar{\Delta} \le R - \sup_{i,j}\{r_{ij}^{max}\}$ defines the maximum reaction gap distance, α and σ are two control parameters, and $\lambda_{ij} = (\mathbf{z}_i - \mathbf{z}_j)^T \dot{\mathbf{z}}_i$ represents the rate at which the ith vehicle either increases ($\lambda_{ij} > 0$) or decreases ($\lambda_{ij} < 0$) its distance to the jth agent. Note that $\Delta_{ij} \to 0$, $R_{ij} \to r_{ij}$ if $\lambda_{ij} \to -\infty$ (i.e., if the ith vehicle is rapidly distancing itself from the jth agent) and $\Delta_{ij} \to \bar{\Delta}$, $R_{ij} \to r_{ij} + \bar{\Delta}$ if $\lambda_{ij} \to -\infty$ (i.e., if the vehicle is fast approaching). The radius

$$R_{ij}^0 =: R_{ij}(0) = r_{ij} + \frac{1}{2}\bar{\Delta} + \frac{1}{\pi}\bar{\Delta}\tan^{-1}(\sigma) \quad (10)$$

denotes the reaction radius when $\lambda_{ij} = 0$. Note that $R_{ij}^0 \equiv R_{ji}^0$, yet R_{ij} and R_{ij} are, in general, not the same. Similarly, $R_{ij} \not\equiv R_{ik}$ for $j \ne k$.

Now, returning to (7) one can show that

$$\frac{\partial V_{ij}^T}{\partial \mathbf{z}_i} = \frac{4(R_{ij} - r_{ij}))(\|\mathbf{z}_i - \mathbf{z}_j\|^2 - R_{ij}^2)(\mathbf{z}_i - \mathbf{z}_j)}{(\|\mathbf{z}_i - \mathbf{z}_j\|^2 - r_{ij}^2)^3}$$

$$\frac{\partial V_{ij}}{\partial r_{ij}} = \frac{4\Delta_{ij}(R_{ij}^2 - \|\mathbf{z}_i - \mathbf{z}_j\|^2)(R_{ij}r_{ij} + \|\mathbf{z}_i - \mathbf{z}_j\|^2)}{(\|\mathbf{z}_i - \mathbf{z}_j\|^2 - r_{ij}^2)^3}$$

if $r_{ij} < \|\mathbf{z}_i - \mathbf{z}_j\| \le R_{ij}$, undefined if $\|\mathbf{z}_i - \mathbf{z}_j\| = r_{ij}$, and zero otherwise. Similarly, one can show that

$$\frac{\partial V_{ij}}{\partial \mathbf{z}_i} = \frac{\partial V_{ji}}{\partial \mathbf{z}_i}, \quad \frac{\partial V_{ij}}{\partial \mathbf{z}_i} = -\frac{\partial V_{ij}}{\partial \mathbf{z}_j}, \quad \frac{\partial V_{ij}}{\partial r_{ij}} = \frac{\partial V_{ji}}{\partial r_{ij}}. \quad (11)$$

Theorem 1. *Consider the system in (1) with control law (3) and (6). Assume that $\mathbf{z}_i^d$ is constant and that $\|\mathbf{z}_i(0) - \mathbf{z}_j(0)\| > r_{ij}\ \forall\ i, j \ne i$. Then, $\|\mathbf{z}_i(t) - \mathbf{z}_j(t)\| > r_{ij}\ \forall\ t \ge 0$.*

Proof. Consider the following Lyapunov function

$$W = \frac{1}{2}\sum_{i=1}^{N}\left(K_p\|\mathbf{z}_i^d - \mathbf{z}_i\|^2 + \|\dot{\mathbf{z}}_i\|^2 + \sum_{i=1}^{N}\sum_{j \in N_i}V_{ij}^0\right). \quad (12)$$

Differentiating (12) with respect to time yields

$$\dot{W} = \sum_{i=1}^{N} \left(-K_p(\mathbf{z}_i^d - \mathbf{z}_i)^T \dot{\mathbf{z}}_i + (K_p(\mathbf{z}_i^d - \mathbf{z}_i) - K_v \dot{\mathbf{z}}_i)^T \dot{\mathbf{z}}_i \right)$$
$$- \sum_{i=1}^{N} \sum_{j \in N_i} \left(\frac{\partial V_{ij}^T}{\partial \mathbf{z}_i} + \frac{\partial V_{ij}^0}{\partial r_{ij}} \frac{\partial r_{ij}}{\partial \mathbf{z}_i}^T + \frac{1}{L_i} \frac{\partial V_{ij}^0}{\partial r_{ij}} \frac{\partial r_{ij}}{\partial \phi_i} \begin{bmatrix} -\sin\phi_i \\ \cos\phi_i \end{bmatrix} \right)^T \dot{\mathbf{z}}_i$$
$$+ \frac{1}{2} \sum_{i=1}^{N} \sum_{j \in N_i} \left(\frac{\partial V_{ij}^0}{\partial \mathbf{z}_i} \dot{\mathbf{z}}_i + \frac{\partial V_{ij}^0}{\partial r_{ij}} \frac{\partial r_{ij}}{\partial \mathbf{z}_i} \dot{\mathbf{z}}_i + \frac{\partial V_{ij}^0}{\partial r_{ij}} \frac{\partial r_{ij}}{\partial \phi_i} \dot{\phi}_i \right)$$
$$+ \frac{1}{2} \sum_{i=1}^{N} \sum_{j \in N_i} \left(\frac{\partial V_{ij}^0}{\partial \mathbf{z}_j} \dot{\mathbf{z}}_j + \frac{\partial V_{ij}^0}{\partial r_{ij}} \frac{\partial r_{ij}}{\partial \mathbf{z}_j} \dot{\mathbf{z}}_j + \frac{\partial V_{ij}^0}{\partial r_{ij}} \frac{\partial r_{ij}}{\partial \phi_j} \dot{\phi}_j \right) \quad (13)$$

Now, canceling the first two terms and noting that

$$\sum_{i=1}^{N} \sum_{j \in N_i} \left(\frac{\partial V_{ij}^0}{\partial \mathbf{z}_i} \dot{\mathbf{z}}_i + \frac{\partial V_{ij}^0}{\partial r_{ij}} \frac{\partial r_{ij}}{\partial \mathbf{z}_i} \dot{\mathbf{z}}_i + \frac{\partial V_{ij}^0}{\partial r_{ij}} \frac{\partial r_{ij}}{\partial \phi_i} \dot{\mathbf{z}}_i \right)$$
$$= \frac{1}{2} \sum_{i=1}^{N} \sum_{j \in N_i} \left(\frac{\partial V_{ij}^0}{\partial \mathbf{z}_i} \dot{\mathbf{z}}_i + \frac{\partial V_{ij}^0}{\partial r_{ij}} \frac{\partial r_{ij}}{\partial \mathbf{z}_i} \dot{\mathbf{z}}_i + \frac{\partial V_{ij}^0}{\partial r_{ij}} \frac{\partial r_{ij}}{\partial \phi_i} \dot{\phi}_i \right.$$
$$\left. + \frac{\partial V_{ij}^0}{\partial \mathbf{z}_j} \dot{\mathbf{z}}_j + \frac{\partial V_{ij}^0}{\partial r_{ij}} \frac{\partial r_{ij}}{\partial \mathbf{z}_j} \dot{\mathbf{z}}_j + \frac{\partial V_{ij}^0}{\partial r_{ij}} \frac{\partial r_{ij}}{\partial \phi_j} \dot{\phi}_j \right) \quad (14)$$

along with $\dot{\phi}_i = \frac{1}{L_i}[-\sin\phi_i, \cos\phi_i]\dot{\mathbf{z}}_i$, yields

$$\dot{W} = -K_v \sum_{i=1}^{N} \|\dot{\mathbf{z}}_i\|^2 - \sum_{i=1}^{N} \sum_{j \in N_i} \left(\frac{\partial V_{ij}}{\partial \mathbf{z}_i} - \frac{\partial V_{ij}^0}{\partial \mathbf{z}_i} \right) \dot{\mathbf{z}}_i$$
$$\leq - \sum_{i=1}^{N} \sum_{j \in N_i} \Lambda_{ij} \lambda_{ij} \quad (15)$$

where

$$\Lambda_{ij} = 4 \frac{(R_{ij}^2 - r^2)(\|\mathbf{x}_i - \mathbf{x}_j\|^2 - R_{ij}^2)}{(\|\mathbf{x}_i - \mathbf{x}_j\|^2 - r^2)^3}$$
$$- 4 \frac{(R_0^2 - r^2)(\|\mathbf{x}_i - \mathbf{x}_j\|^2 - R_0^2)}{(\|\mathbf{x}_i - \mathbf{x}_j\|^2 - r^2)^3}. \quad (16)$$

Note that if $\lambda_{ij} \geq 0$, then $R_{ij} \leq R_0$, which implies that $\Lambda_{ij} \geq 0$ and, hence $\Lambda_{ij}\lambda_{ij} \geq 0$. Similarly, if $\lambda_{ij} < 0$, then $R_{ij} > R_0 \Rightarrow \Lambda_{ij} < 0 \Rightarrow \Lambda_{ij}\lambda_{ij} > 0$. Therefore, $\dot{W} \leq 0$ for all $t \geq 0$. The latter implies that $W(t)$ is non-increasing and bounded $\forall\, t \geq 0$. Now, suppose that for some pair $i, j \neq i$ one have that $\|\mathbf{z}_i(t) - \mathbf{z}_j(t)\| \to r_{ij}$ for some $t > 0$. The latter would imply that $W(t) \to \infty$, which is a contradiction. Since the solutions of (4a) are continuous, one must have that $\|\mathbf{z}_i(t) - \mathbf{z}_j(t)\| \nrightarrow r_{ij}$ for all $i, j \in N_i, t > 0$ and the proof is complete. □

Theorem 1 guarantees that if all agents start at a safe distance from each other, they will remain at a safe distance for all time. Note that it does not say anything about convergence to the agents' desired positions. Results on convergence are given next.

Theorem 2. *Assume that $\mathbf{z}_i^d$ is constant and that $\|\mathbf{z}_i(0) - \mathbf{z}_j(0)\| > r_{ij} \,\forall\, i, j \neq i$. Then, $\mathbf{z}_i - \mathbf{z}_i^d$, $\dot{\mathbf{z}}_i$ and $\dot{\phi}_i$ are uniformly ultimately bounded (UUB). Furthermore, if $\exists T_0$ such that $\mathbf{u}_i^a = 0 \,\forall\, t \geq T_0$, then $\mathbf{z}_i - \mathbf{z}_i^d$, $\dot{\mathbf{z}}_i$ and $\dot{\phi}_i$ vanish exponentially as $t \to \infty$.*

Proof. From Theorem 1 one have that W is bounded, which implies that V_{ij} and V_{ij}^0 are also bounded $\forall\, i, j \neq i, t \geq 0$. Boundedness of V_{ij} and V_{ij}^0, along with the fact that r_{ij} is continuously differentiable with bounded derivative by construction, implies that $\exists \bar{u} < \infty$ such that $\mathbf{u}_i^a \leq \bar{u} \,\forall\, i, t \geq 0$. Now, let $\mathbf{e}_i = \mathbf{z}_i^d - \mathbf{z}_i$, $\dot{\mathbf{e}}_i = -\dot{\mathbf{z}}_i$, and $\ddot{\mathbf{e}}_i = -\ddot{\mathbf{z}}_i = -K_p\mathbf{e}_i - K_v\dot{\mathbf{e}}_i - \mathbf{u}_i^a$ be the tracking error, velocities, and accelerations, and consider the following Lyapunov candidate function

$$\mathcal{W} = K_p \|\mathbf{e}_i\|^2 + \frac{1}{2}\|\dot{\mathbf{e}}_i\|^2 + \frac{1}{2}\|\dot{\mathbf{e}}_i - K_v\mathbf{e}_i\|^2. \quad (17)$$

Taking the time derivative of $\mathcal{W}$ yields

$$\dot{\mathcal{W}} = 2K_p\mathbf{e}_i^T\dot{\mathbf{e}}_i + \dot{\mathbf{e}}_i^T\ddot{\mathbf{e}}_i + (\dot{\mathbf{e}}_i + K_v\mathbf{e}_i)^T(\ddot{\mathbf{e}}_i + K_v\dot{\mathbf{e}}_i)$$
$$= -K_v\|\dot{\mathbf{e}}_i\|^2 - K_pK_v\|\mathbf{e}_i\|^2 - 2\dot{\mathbf{e}}_i^T\mathbf{u}_i^a - K_v\mathbf{e}_i^T\mathbf{u}_i^a$$
$$\leq -aK_v\|[\mathbf{e}_i,\dot{\mathbf{e}}_i]^T\|^2 + b\bar{u}\|[\mathbf{e}_i,\dot{\mathbf{e}}_i]^T\| \quad (18)$$

where $a = \min\{1, K_p\}$ and $b = \max\{2, K_v\}$. Since $\dot{\mathcal{W}} < 0$ for all $\|[\mathbf{e}_i,\dot{\mathbf{e}}_i]^T\| > b\bar{u}/(aK_v)$, one can conclude that $[\mathbf{e}_i,\dot{\mathbf{e}}_i]^T$ is UUB (Khalil, 2002), and from (4b), that $\dot{\phi}_i$ is also UUB.

Now, assume that $\exists T_0$ such that $\mathbf{u}_i^a = 0 \,\forall\, t \geq T_0$. Then, $\dot{\mathcal{W}} \leq -aK_v\|[\mathbf{e}_i,\dot{\mathbf{e}}_i]^T\|^2 \,\forall\, t \geq T_0$ from which one can conclude that $[\mathbf{e}_i,\dot{\mathbf{e}}_i]^T$ converges asymptotically to zero. The latter implies that $\dot{\phi}_I \to \mathbf{0}$ as $t \to 0$. □

The theoretical results presented so far guarantee collision avoidance when the desired position is constant and when all agents apply the same control (or remain static). A natural extension is the use of way-points to drive the vehicles through a desired path or trajectory. Additionally, the results presented so far cannot guarantee the convergence of the tracking error to zero in all scenarios, i.e., agents may find themselves trapped in a deadlock. The next section will discuss implementing way-points in the control law and avoiding deadlocks.

3.2 Way-Points and Deadlocks

A main drawback of decentralized APF methods is the occurrence of deadlocks (Melchiorre et al., 2022). A vehicle is said to reach a deadlock if it can not reach the desired position due to a persistent interaction with another agent or obstacle. This is oftentimes the result of symmetries between the attractive potential forces (i.e., the first term in (6)) and the avoidance

control (Rodríguez-Seda et al., 2016). That is, when $\mathbf{u}_i^a \to K_p(\mathbf{z}_i - \mathbf{z}_i^d)$. To break these symmetries, one can temporarily change the desired position along a vector that is perpendicular to the avoidance control.

Consider an ordered sequence of unobstructed M_i way-points, $\mathbf{z}_i^k \in \{\mathbf{z}_i^1, \cdots, \mathbf{z}_i^{M_i}\}$, in the ith vehicle's desired path separated by at least a distance $D_i > 0$ of each other. The idea is to go to the next way-point $\mathbf{z}_i^{k+1}$ whenever the distance of the vehicle to the kth way-point is smaller than some positive parameter $d_i \ll D_i$. Since the agents' velocities are bounded, the times between switches are lower bounded by some positive constant $\tau_i > 0$. The latter is a necessary condition for stability and avoidance of Zeno behavior.

Now, due to the presence of obstacles and other agents, the ith vehicle may not reach the kth way-point and may end up circulating around it for an indefinite time. To escape the deadlock, the vehicle may temporarily switch to a new way-point, $\tilde{\mathbf{z}}_i^k$. The new way-point can be chosen in a direction that is perpendicular to the avoidance control, i.e.,

$$\tilde{\mathbf{z}}_i^k = \mathbf{z}_i + \mu_i \mathcal{R}(\pi/2)\mathbf{u}_i^a, \ \text{if } \left\|\mathbf{u}^a + K_p(\mathbf{z}_i - \mathbf{z}_i^k)\right\| \le U_i \ (19)$$

where μ_i is a non-zero constant parameter, $U_i > 0$ is a small constant, and $\mathcal{R}(\pi/2)$ is the 2×2 rotational matrix that rotates $\mathbf{u}_i^a$ by $\pi/2$ radians. This temporary way-point can last for a pre-determined amount of time T_i in order to avoid multiple switching in a short time frame. After T_i, the vehicle may go back to the original way-point $\mathbf{z}_i^k$ or switch to another way-point using (19) if the conflict has not been resolved. The complete algorithm is given in Algorithm 1.

4 EXAMPLES

This section presents examples of vehicles of rectangular shape with rectangular and circular obstacles.

4.1 Minimum Safe Distance

Let the shape of the ith vehicle be approximated by a rectangle of length ℓ_i and width w_i. Similarly, let the jth vehicle or obstacle be approximated by a rectangle of length ℓ_j and width w_j. Without loss of generality, let their lengths be aligned with the x-axis (i.e., when $\phi_i = 0$) and define the following functions

$$\beta_{ij} = \frac{\ell_i}{2} + \frac{\ell_j}{2}\sqrt{\varepsilon^2 + \cos^2 \tilde{\phi}_{ij}} + \frac{w_j}{2}\sqrt{\varepsilon^2 + \sin^2 \tilde{\phi}_{ij}} \ (20a)$$

$$\gamma_{ij} = \frac{w_i}{2} + \frac{\ell_j}{2}\sqrt{\varepsilon^2 + \sin^2 \tilde{\phi}_{ij}} + \frac{w_j}{2}\sqrt{\varepsilon^2 + \cos^2 \tilde{\phi}_{ij}} \ (20b)$$

where $\varepsilon > 0$ is a small constant such that the derivatives of (20) are well-defined and $\tilde{\phi}_{ij} = \phi_i - \phi_j$ is the

---

Algorithm 1: Way-Point Selection.

Constants: $d_i, U_i, K_p, \mu_i, T_i, M_i$
Input: $k, \mathbf{z}_i, \mathbf{u}_i^a, \mathbf{z}_i^k, \mathbf{z}_i^{k+1}$
Output: $\mathbf{z}_i^d, k$
if $k < M_i$ **and** $\left\|\mathbf{z}_i - \mathbf{z}_i^k\right\| < d_i$ **:**
  $\quad \mathbf{z}_i^d \leftarrow \mathbf{z}_i^{k+1}$ $\qquad$ /* Pick Next Way-Point */
  $\quad k \leftarrow k + 1$
else if $\left\|\mathbf{z}_i - \mathbf{z}_i^k\right\| \ge d_i$ **and** $\left\|\mathbf{u}_i^a + K_p(\mathbf{z}_i - \mathbf{z}_i^k)\right\| \le U_i$ **:**
  $\quad \tilde{\mathbf{z}}_i^k \leftarrow \mathbf{z}_i + \mu_i \mathcal{R}(\pi/2)\mathbf{u}_i^a$
  $\quad t^\star \leftarrow t$
  $\quad$ **while** $t \le t^\star + T_i$ **do**
  $\quad\quad \mathbf{z}_i^d \leftarrow \tilde{\mathbf{z}}_i^k$ $\qquad$ /* Switch temporarily */
else:
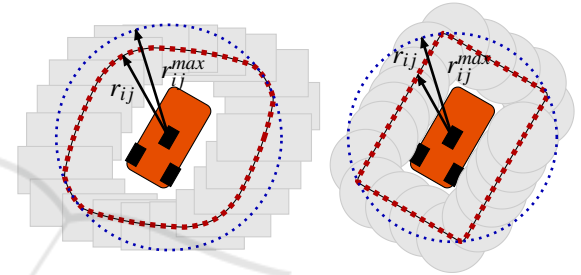 $\quad \mathbf{z}_i^d \leftarrow \mathbf{z}_i^k$

Figure 2: Comparison of the minimum safe distance between the proposed control framework (in red) and the traditional circular assumption (in blue). The left figure illustrates the case when the vehicle and obstacle have a rectangular shape. The right figure depicts the case when the obstacle has a circular shape.

relative orientation. Let $\theta_{ij} = \text{atan2}(z_{j,2} - z_{i,2}, z_{j,1} - z_{i,1})$ be the angle between $\mathbf{z}_i$ and $\mathbf{z}_j$. Then, the equation for a rectangle with sides β_{ij} and γ_{ij} in polar coordinates ρ_{ij} and θ_{ij}, rotated by ϕ_i and centered at $\mathbf{z}_i$ can be approximated by

$$\zeta_{ij} = \sqrt{\varepsilon^2 + (\gamma_{ij}\cos(\theta_{ij} - \phi_i) + \beta_{ij}\sin(\theta_{ij} - \phi_i))^2} \ (21a)$$

$$\eta_{ij} = \sqrt{\varepsilon^2 + (\gamma_{ij}\cos(\theta_{ij} - \phi_i) - \beta_{ij}\sin(\theta_{ij} - \phi_i))^2} \ (21b)$$

$$\rho_{ij} = \frac{2\beta_{ij}\gamma_{ij}}{\zeta_{ij} + \eta_{ij} - 2\varepsilon}. \ (21c)$$

Following the same procedure for the jth agent and using the continuous differentiable approximation of the minimum function (Stipanović et al., 2012), one can obtain a smooth approximation of r_{ij}

$$r_{ij} = r_{ji} = (2)^{\frac{1}{\delta}}\left(\rho_{ij}^{-\delta} + \rho_{ji}^{-\delta}\right)^{-\frac{1}{\delta}}, \quad \delta \ge 2 \quad (22)$$

that is continuously differentiable and bounded. Choosing smaller $\varepsilon \to 0$ and larger $\delta \to \infty$ yields more compact envelopes. The left side of Figure 2 illustrates r_{ij} for different relative positions between two rectangular agents of different sizes and different ori-
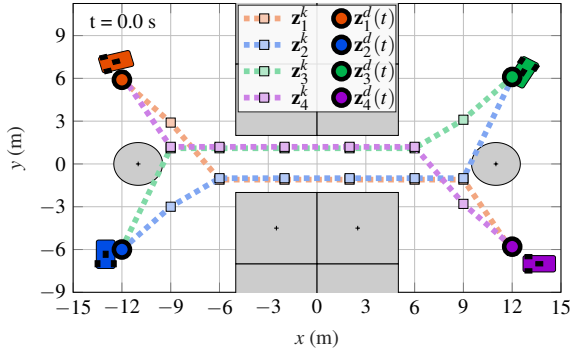
Figure 3: Simulated scenario with four vehicles and several static obstacles represented as squares and circles.

entations. The red-dotted line represents the minimum safe distance that the center of the jth agent can come from the ith vehicle, which is generally shorter than the constant minimum distance scenario.

The case of an obstacle of circular shape can be similarly addressed. Consider an obstacle with radius h_j. The rectangle obtained by moving the circular obstacle around the vehicle as seen in Figure 2 has half-length $\ell_{ij} = \frac{1}{2}\ell_i + h_j$ and half-width $w_{ij} = \frac{1}{2}w_i + h_j$. Then, similar to (21), one can define this rectangle in polar coordinates r_{ij} and $\theta_{ij} = \operatorname{atan2}(z_{j,2} - z_{i,2}, z_{j,1} - z_{i,1})$, where r_{ij} is given by

$$q_{ij} = \sqrt{\varepsilon^2 + (w_{ij}\cos(\theta_{ij} - \phi_i) + \ell_{ij}\sin(\theta_{ij} - \phi_i))^2} \quad (23a)$$

$$s_{ij} = \sqrt{\varepsilon^2 + (w_{ij}\cos(\theta_{ij} - \phi_i) - \ell_{ij}\sin(\theta_{ij} - \phi_i))^2} \quad (23b)$$

$$r_{ij} = r_{ji} = \frac{2w_{ij}\ell_{ij}}{q_{ij} + s_{ij} - 2\varepsilon}. \quad (23c)$$

Figure 2 illustrates r_{ij} for different relative orientations between the ith vehicle and the jth agent.

4.2 Simulations

Consider a group of four identical vehicles (1) of rectangular shape, with length $\ell_i = 2$ m and width $w_i = 1$ m, traveling through a highly obstructed environment, as shown in Figure 3. Each vehicle is tasked with following a series of way-points by implementing (6) and Algorithm 1. The system and control parameters are given as $m_i = 1$ Kg, $J_i = 1$ Kg m^2, $K_p = 1$ N/m, $K_v = 2$ Ns/m, $L_i = 2/3$ m, $D_i = 1.5$ m, $U_i = 0.2$ N, and $\mu_i = 2\sqrt{2}$ N, $\bar{\Delta} = 4$ m, $\alpha = 0.4$, $\sigma = -0.3$, $\delta = 6$, and $\varepsilon = 0.05$. The static obstacles are assumed to be squares of side $\ell_j = w_j = 5$ m, while circular obstacles have radius $h_j = 1.5$ m.

The response of the multi-vehicle system is given in Figure 4. The vehicles are able to follow the way-points and navigate smoothly through the narrow corridor while avoiding collisions and deadlocks, despite
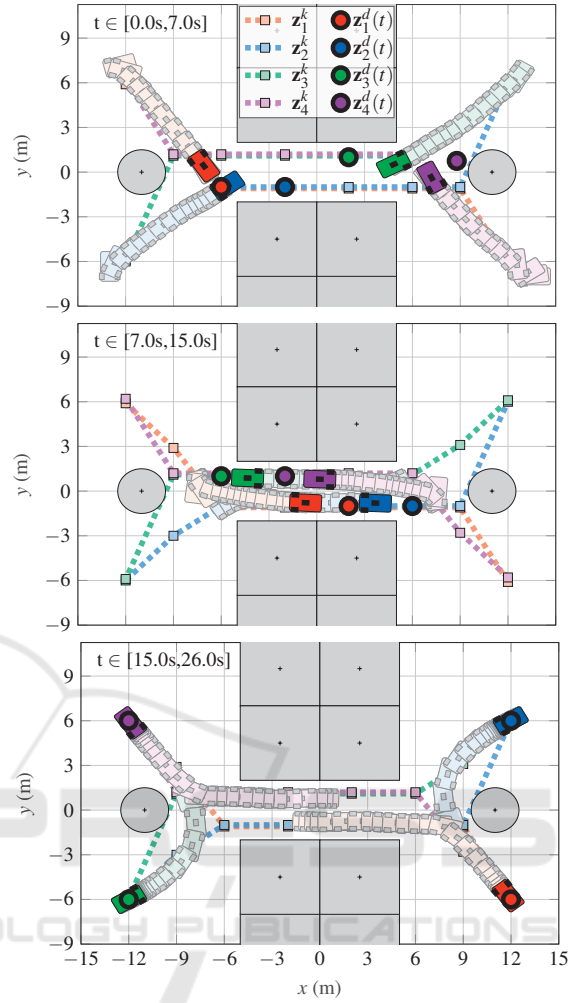

Figure 4: Sequential motion of the multi-vehicle system under proposed avoidance control. Newer positions are over-imposed and time-spaced by 0.5 s.

having symmetric desired paths with obstacles in their way. Note also that the leading vehicles, 2nd and 3rd, are able to avoid the last circular obstacles in their paths while being closely followed by another agent.

For comparison, the vehicles are also simulated using the proposed control law (7) but with a constant reaction gap distance of $\Delta_{ij} = \Delta_{ij}(0) = 0.41$ m. This approach is equivalent to the one proposed in (Rodríguez-Seda, 2024b). The results are presented in Figure 5. Note that, for the first 15 s, the vehicles' response is very similar to the previous case. However, once the vehicles reach the last obstacles and are encircled by another vehicle closely behind, the second and third vehicles experience a forceful reaction that leads them outside of the plotted area. This is due to the smaller reaction gap, which requires more drastic maneuvers in order to avoid collisions.

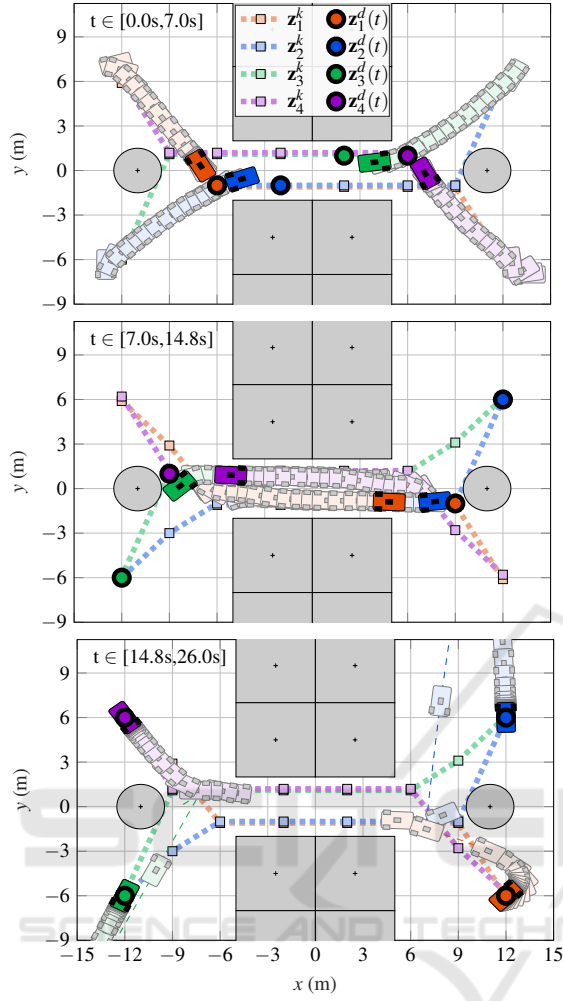Finally, the multi-vehicle system is also simulated

Figure 5: Sequential motion of the multi-vehicle system with constant detection gap distance. Newer positions are over-imposed and time-spaced by 0.5 s.

Figure 6: Sequential motion of the multi-vehicle system with constant minimum safe distance and constant reaction gap distance.

using a constant minimum safe distance radius and a constant reaction gap distance of $\Delta_{ij} = 0.41$ m. When avoiding other vehicles, the minimum safe distance is chosen as the sum of their circumradii, i.e., $r_{ij} = r_{ji} = h_i + h_j = 2\sqrt{2}$ m. For circular obstacles, it is chosen as $r_{ij} = h_i + h_j = \sqrt{2} + 1.5$ m. All other obstacles are divided into smaller 2.5×2.5 m^2 squares to allow the transit of vehicles over the narrow corridor. For these obstacles, r_{ij} is chosen as $r_{ij} = 2.25\sqrt{2}$ m. Note that, since r_{ij} is constant, the avoidance control reduces to $\mathbf{u}_i^a = -\sum_{j \in N_i} \partial V_{ij}^0 / \partial \mathbf{z}_i$, which is the traditional APF approach. The results are illustrated in Figure 6. Note that the vehicles are able to enter the narrow corridor, where they reach a deadlock. The $\mathbf{z}_i^d = \tilde{\mathbf{z}}_i^k$ points outside the desired path illustrate how the vehicles try to evade the deadlock but are unsuccessful.

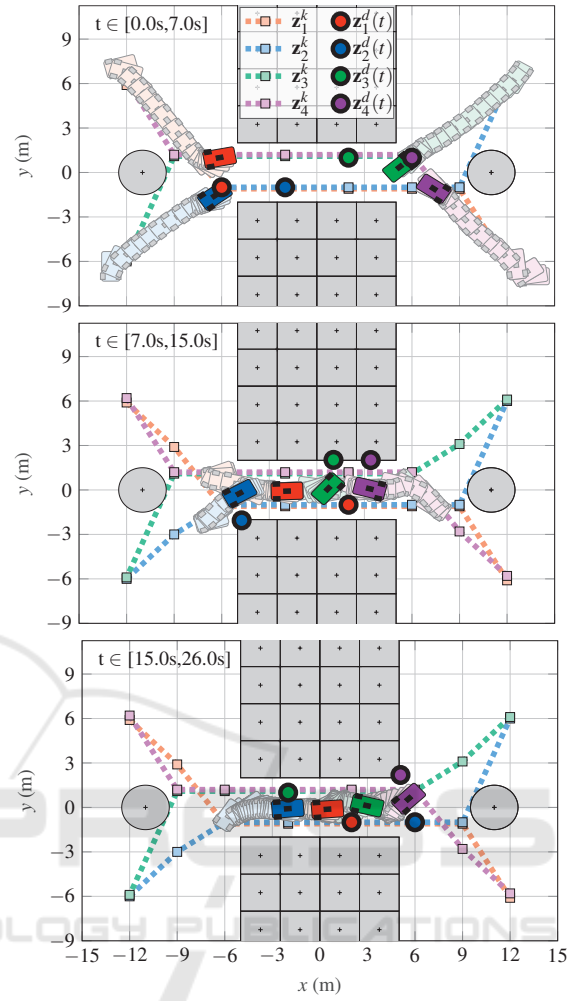Figures 7, 8, and 9 show the cumulative instantaneous error, force, and torque for the case of the proposed controller (Proposed Control), the case of a constant reaction gap (Constant Δ_{ij}), and for the case of a constant minimum safe distance and reaction gap (Constant r_{ij} and Δ_{ij}). Note that errors are, in general, smaller for the proposed avoidance control. Similarly, note that the forces and torques are, in general, one and four orders in magnitude larger for the use of constant reaction gaps.

5   CONCLUSIONS

This paper presented a decentralized, cooperative, APF-based control framework for multi-vehicle systems of unicycle type that is rigorously proven to guarantee collision avoidance for an arbitrarily large number of agents at all times. The control framework defines a continuously differentiable time-varying
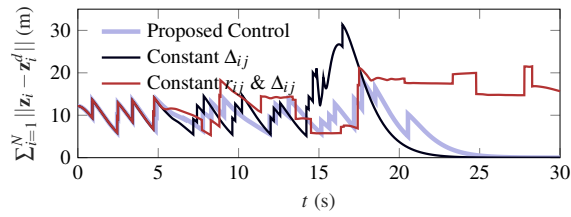
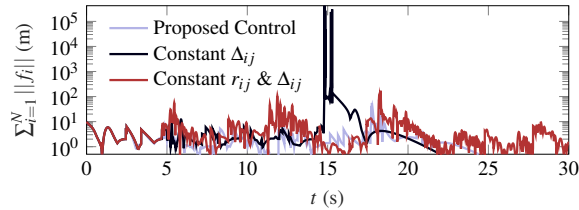Figure 7: Cumulative tracking error.

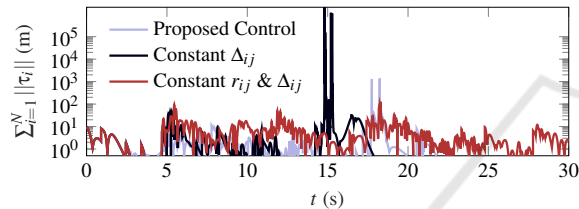Figure 8: Cumulative linear force (in logarithm scale).

Figure 9: Cumulative torque (in logarithm scale).

minimum safe distance that agents need to enforce, taking into consideration the shape and orientation of vehicles and obstacles and, therefore, reducing the conservatism introduced by traditional APF-based methods. Furthermore, the framework modulates the avoidance maneuvers and reaction forces based on the collision threat level that obstacles might represent. The synthesis of both approaches is a continuously smooth and bounded control force provided in analytical closed-form. Simulation results demonstrated that the proposed avoidance control can increase the maneuverability of vehicles through highly constrained spaces when compared to the use of constant minimum safe distance and reaction radii.

REFERENCES

Braquet, M. and Bakolas, E. (2022). Vector field-based collision avoidance for moving obstacles with time-varying elliptical shape. In *Proc. AACC MECC*, pages 587–592.

Brockett, R. W. (1983). Asymptotic stability and feedback stabilization. In Brockett, R. W., Millman, R. S., and Sussmann, H. J., editors, *Differential Geometric Control Theory*, pages 181–191. Birkhauser, Boston.

Du, Y., Zhang, X., and Nie, Z. (2019). A real-time collision avoidance strategy in dynamic airspace based on dynamic artificial potential field algorithm. *IEEE Access*, 7:169469–169479.

Gao, Y., Li, D., et al. (2024). Trajectory planning and tracking control of autonomous vehicles based on improved artificial potential field. *IEEE Trans. Veh. Technol.*, pages 1–16.

Ginesi, M., Meli, D., et al. (2021). Dynamic movement primitives: Volumetric obstacle avoidance using dynamic potential functions. *J. Intell. Robot. Syst.*, 101:1–20.

Hoy, M., Matveev, A. S., and Savkin, A. V. (2014). Algorithms for collision-free navigation of mobile robots in complex cluttered environments: A survey. *Robotica*, 33(3):463–497.

Khalil, H. K. (2002). *Nonlinear Systems*. Prentice Hall, New Jersey.

Khatib, O. (1986). Real-time obstacle avoidance for manipulators and mobile robots. *Int. J. Robot. Res.*, 5(1):90–98.

Melchiorre, M., Scimmi, L. S., et al. (2022). Robot collision avoidance based on artificial potential field with local attractors. In *Proc. ICINCO*, pages 340–350.

Raibail, M., Rahman, A. H. A., et al. (2022). Decentralized multi-robot collision avoidance: A systematic review from 2015 to 2021. *Symmetry*, 14(3).

Rodríguez-Seda, E. J. (2024a). Decentralized low-energy avoidance control framework for multiple mobile agents using irregular observations. *IEEE Trans. Control Syst. Technol.*, 32(3):1027–1039.

Rodríguez-Seda, E. J. (2024b). Reactive collision avoidance control for nonholonomic vehicles and obstacles of arbitrary shape. *ASME. Letters Dyn. Sys. Control*, 4(3):031005.

Rodríguez-Seda, E. J., Stipanović, D. M., and Spong, M. W. (2016). Guaranteed collision avoidance for autonomous systems with acceleration constraints and sensing uncertainties. *J. Optim. Theory Appl.*, 168(3):1014–1038.

Rodríguez-Seda, E. J. and Stipanović, D. M. (2020). Cooperative avoidance control with velocity-based detection regions. *IEEE Control Syst. Lett.*, 4(2):432–437.

Rodríguez-Seda, E. J., Tang, C., et al. (2014). Trajectory tracking with collision avoidance for nonholonomic vehicles with acceleration constraints and limited sensing. *Int. J. Robot. Res.*, 33(12):1569–1592.

Stipanović, D. M., Hokayem, P. F., et al. (2007). Cooperative avoidance control for multiagent systems. *J. Dyn. Syst. Meas. Control*, 129:699–707.

Stipanović, D. M., Tomlin, C. J., and Leitmann, G. (2012). Monotone approximations of minimum and maximum functions and multi-objective problems. *Appl. Math. Optim.*, 66(3):455–473.

Xiao, X., Liu, B., et al. (2021). Toward agile maneuvers in highly constrained spaces: Learning from hallucination. *IEEE Rob. Autom. Lett.*, 6(2):1503–1510.

Zhang, W., Rodríguez-Seda, E. J., et al. (2020). Avoidance control with relative velocity information for lagrangian dynamics. *J. Intell. Robot. Syst.*, 99:229–244.

Zimmermann, S., Busenhart, M., et al. (2022). Differentiable collision avoidance using collision primitives. In *Proc. IEEE/RSJ Int. Conf. Intell. Robots Syst.*, pages 8086–8093.